THE ASTROPHYSICAL JOURNAL, 210:733–740, 1976 December 15

SOME COMPARISONS OF THEORETICAL SUPERNOVA LIGHT CURVES WITH SUPERNOVA 1969l (TYPE II) IN NGC 1058

W. DAVID ARNETT
University of Illinois at Urbana-Champaign; and Enrico Fermi Institute, University of Chicago

AND

SYDNEY W. FALK
Kellogg Radiation Laboratory, California Institute of Technology
Received 1976 March 18; revised 1976 May 24

ABSTRACT

Using the empirical transformations of Kirshner and Kwan, we compare the *UBV* photometry of Ciatti, Rosino, and Bertola for Type II supernova SN 1969l in NGC 1058 with the theoretical predictions of Falk and Arnett. Spectra and spectral scans by these observers are used to infer fluid velocities. The behavior as a function of time of (1) the effective temperature, (2) the fluid velocity, and (3) the photospheric radius is compared in detail. The only adjustment made is to synchronize the observational and theoretical times at maximum effective temperature. The agreement is good.

Subject headings: galaxies: individual — stars: supernovae

I. INTRODUCTION

In an earlier paper (Falk and Arnett 1973) we presented a model for light curves of Type II supernovae. Although Ciatti, Rosino, and Bertola (1971) had recently published extensive *UBV* photometry of the bright Type II supernova 1969l in NGC 1058, we were unable to make detailed comparisons of our theoretical calculations with their observational results. Our computational scheme approximated the photon spectrum by a blackbody (see Christy 1964; Falk and Arnett 1976 for details), so that a transformation of *UBV* photometry to an effective temperature scale was necessary. Blindly using conversions derived from stellar calibration seemed unreliable to us. However, since our work was published Kirshner and Kwan (1974) have used detailed spectral scans of that supernova to empirically derive a *UBV* to T_e conversion. Because (1) these models predict rather than describe the observational results (they were calculated prior to the data becoming available), (2) these models agree well with the observations, (3) these models represent a simple and clear form of theoretical calculations of this type, and (4) these models have been described incompletely before, we add to our previous discussion. In this paper we restrict our scope to the following: we compare the predictions of our old calculations to the newly inferred characteristics of SN 1969l. For a detailed analysis of much of the physics relevant to such models, see Falk and Arnett (1976). For references to the growing literature on blast-wave–radiative-diffusion models of Type II supernovae, see Falk and Arnett (1973, 1976) and Chevalier (1976), for example.

The nature of the calculations was briefly described by Falk and Arnett (1973). A computational method for explicit hydrodynamics and implicit radiative transfer similar to that of Christy (1964) was used. The validity of approximating the transfer equation by an equilibrium diffusion equation has been examined (Falk 1974; Falk and Arnett 1976); the approximation appears adequate for purposes of this paper. Our nonequilibrium calculations give similar results, at least in the gray approximation (see Falk and Arnett 1976). The equilibrium diffusion approach does not give details of line formation; this requires additional analysis and assumptions. In this paper we discuss only the general character of the spectrum as given by its effective temperature. For a preliminary discussion of line formation see Kirshner and Kwan (1975).

The characteristics of the two initial models are summarized in Table 1. The opacity was essentially the Cox-Stewart (1965) Rosseland mean opacity for a Population I (i.e., solar) composition. The inner zone was given a kinetic energy to mock up an explosion. As the evolution proceeds, a shock wave develops, blowing the star apart. This input energy ($E = 3 \times 10^{50}$ to 10^{51} ergs) was obtained from estimates of the energy needed to give the observed characteristics of supernova remnants (especially X-ray emission). For these initial models this choice naturally gives an optical output close to that observed for Type II supernovae.

The structure of the "red-giant" part of the presupernova star was obtained by modeling some envelope integrations of Paczynski (1969). The circumstellar shell was of constant density.

TABLE 1

CHARACTERISTIC OF THE INITIAL MODELS

Model	Mass ($M_\odot$)	Radius (cm)	Energy Added (ergs)	Comments
A*..........	10	1.6×10^{14}	10^{51}	No shell; "surface" density is $\rho \approx 5 \times 10^{-9}$ g cm^{-3}; scaled from Paczynski envelope
B*..........	10	9.6×10^{14}	$10^{50.5}$	Extensive (3 $M_\odot$) shell around a "Paczynski" envelope; shell density is $\rho \approx 10^{-12}$ g cm^{-3}

* Both models had a solar composition.

II. RESULTS

a) History of the Effective Temperature

The development in time of the observed effective temperature is important because it is independent of the estimated distance to the supernova. It is also interesting because a correct prediction of this behavior is a first step toward understanding the changes of the spectrum with time.

From Kirshner and Kwan (1974) we take the effective temperature T_e to be related to the *UBV* photometry of Ciatti, Rosino, and Bertola (1971) by

$$10{,}000\ \mathrm{K}/T_e = 1.59\,(B - V) + 0.48\,.$$

Using the *UBV* photometry of Ciatti, Rosino, and Bertola (1971), we obtain T_e as a function of time for SN 1969l. This is shown in Figure 1. The closed circles represent the points given by Kirshner and Kwan (1974) in their Table 4. The open circles represent

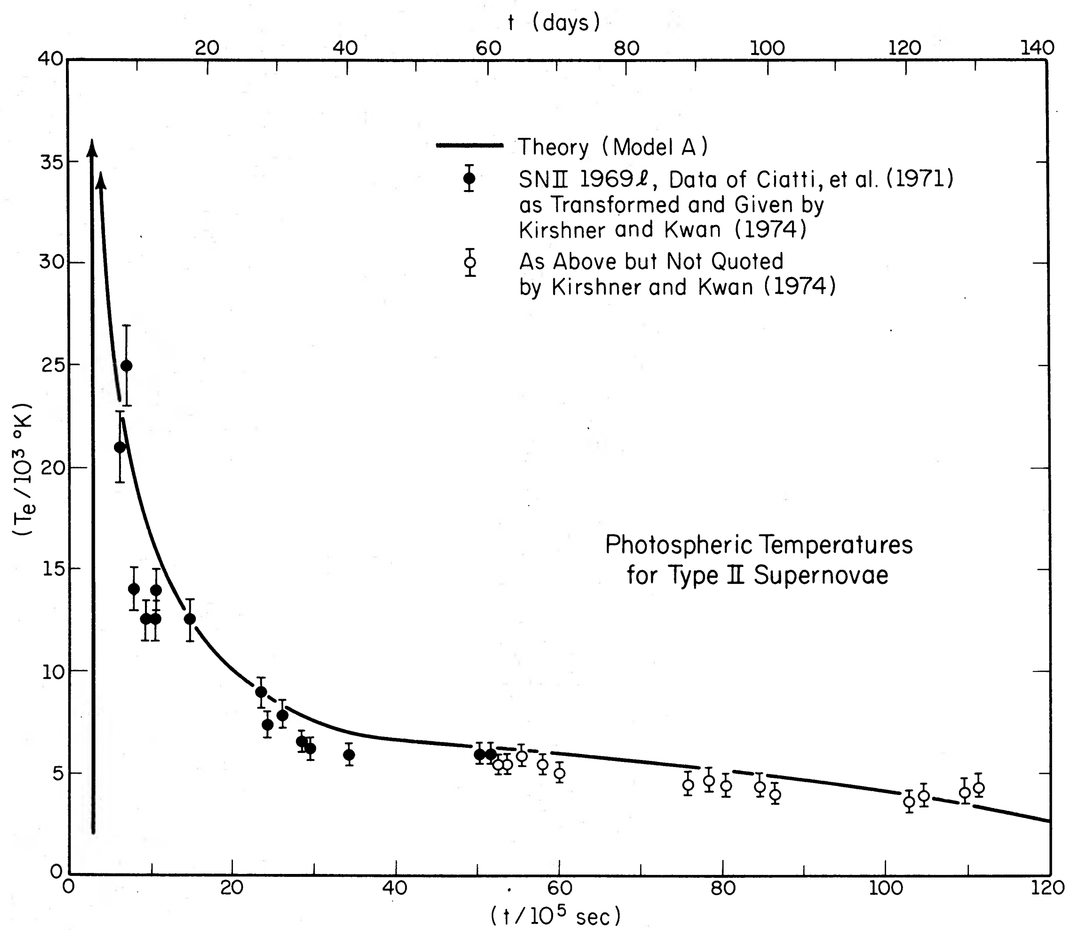

FIG. 1.—Photospheric temperatures T_e for Type II supernovae as a function of time. The solid line is the prediction of Model A of Falk and Arnett (1973). The solid data points are from the photometry of Ciatti *et al.* (1971) and reduced to an effective temperature scale by Kirshner and Kwan (1974). The open data points are also from Ciatti *et al.* (1971), reduced to T_e with the same transformation by the authors of this paper. The theoretical and observational times were synchronized at maximum T_e.

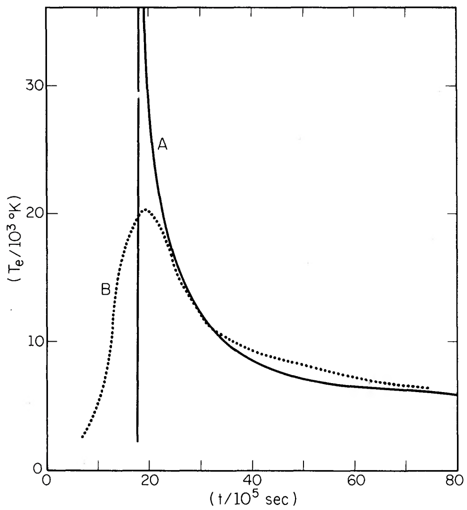

FIG. 2.—Photospheric temperatures T_e for models A and B. Model B (*dotted curve*) differs from A (*solid curve*) primarily by the addition of an extended circumstellar shell. After peak T_e the curves differ little.

additional data they did not list. The error bars are derived from error estimates given by Kirshner and Kwan (1974). The earliest spectral scan that they had corresponded to $T_e \approx 12{,}000$ K. For the earlier points the *UBV* to T_e conversion is only an extrapolation. At very late times there are other problems (see below). Our approach is to take the empirical conversion at face value and hope that better observational results will be forthcoming. The solid line in Figure 1 represents the predicted T_e from model A. The zero of the time coordinate for the observational data was chosen so the high-temperature points would coincide. No other adjustment was made.

We feel that this agreement is startlingly good. To what extent is this agreement unique? Many other possibilities remain to be tried, but some information can be gleaned from the behavior of T_e in model B. Figure 2 shows this behavior (*dotted line*) compared with that of model A (*solid line*). The two curves are not too different past the maximum in temperature. To the extent we can believe the two high-temperature points, they seem to suggest model A is preferable. Also in the range $3.5 \leq t/10^6\ \mathrm{s} \leq 7$, model A is slightly better. It would be premature to rule out models of type B on the basis of these curves alone even if there were no observational error. First, our theoretical modeling of the optical burst is not yet satisfactory (see below). Second, a thorough survey using many variations in parameters (e.g., explosion energy, mass, extent, structure, composition, etc.) has not yet been done. It seems fair to say that models of type A look slightly better *for SN 1969l*, and the overall agreement of both models with the observations of $T_e(t)$ is promising. However, the behavior of the *photospheric radius* (see below) suggests that model A is to be preferred for this event.

b) *Doppler Shifts*

Doppler shifts of absorption lines give the velocity of matter at varying depths (depending on the line in question) in the photosphere of the supernova. Our calculations give predictions of the velocity of matter at, say, optical depth $\tau = 1$, which may be compared directly with the absorption-line data. Estimates of the behavior of emission lines are not so easy and will not be attempted here.

Figure 3 shows the inferred expansion velocities from the line identifications and Doppler shift measurements of Ciatti, Rosino, and Bertola (1971). The dots representing the data for a given absorption feature are connected. At first the photosphere is in the outer, fast-moving matter; but as this becomes tenuous the inner, slower-moving material is seen. The theoretical prediction for model A is shown by a curve which is partly dotted and partly solid. Our calculations use finite-sized mass zones; we interpolate to find the matter velocity at the point where the optical depth is $\tau = 1$. This works well so long as several mass zones are in the region of interest. The dotted line represents a stage at which the $\tau = 1$ layer was in the *outermost single zone*. For this part of the curve our mathematics was not adequate to predict the photospheric velocity accurately (see the next section below, however).

Our techniques are valid for the part of the curve given by a solid line. Note that the magnitude and slope of this part of the curve agree nicely with the observations.

To what extent does this agreement depend on the uncertainties of line identification? To test this, a similar plot was constructed using Doppler shift measurements and line identifications of Kirshner and Kwan (1974). All of their absorption lines which had enough data to establish a curve for $t \leq 1.2 \times 10^6$ s were used. The results are shown in Figure 4. As may

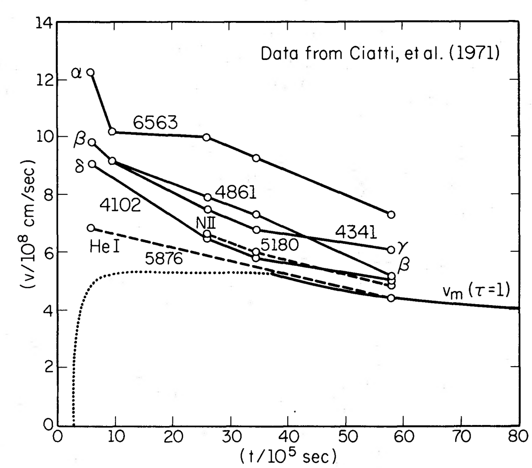

FIG. 3.—Doppler velocities of absorption lines compared to fluid velocities. The observational data are from Ciatti *et al.* (1971). The fluid velocity v_m at optical depth $\tau = 1$ for model A is shown. The dotted portion of the curve is artificially low due to crude mass zoning (see text for details). Curves for smaller τ would be displaced to higher velocity.

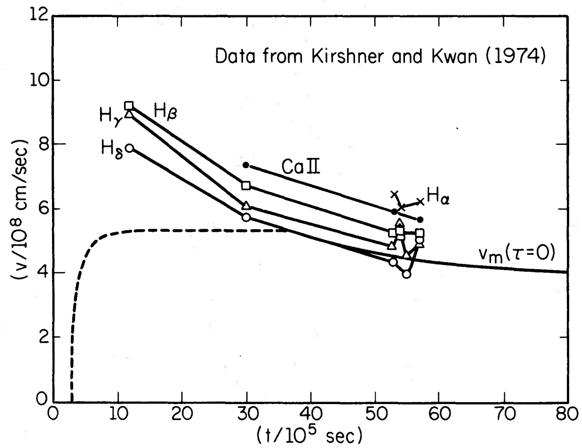

FIG. 4.—Doppler velocities of absorption lines compared with fluid velocities. This differs from Fig. 3 only in that the data and identifications of Kirshner and Kwan (1974) are used. The basic agreement between theory and observation is insensitive to disagreement between these sets of authors on line identification.

easily be seen, the results are virtually identical for our purposes.

c) *Spherically Symmetric Shock Waves*

What should the earlier behavior be? If the photon diffusion can be neglected, then the standard solutions for a strong shock in a decreasing density gradient may be used. Zel'dovich and Raizer (1967) give a clear discussion of the physical meaning of these solutions as well as references to the original papers. When is this approximation valid? Consider a region of characteristic dimension ΔR. The time scale for diffusion across ΔR is $\tau \approx 3(\Delta R)^2/\lambda c$, where λ is the mean free path and c the velocity of the diffusing particles. Roughly speaking, we may define a "diffusion velocity" v_d by $v_d \approx \Delta R/\tau = \lambda c/3\Delta R$. If $v_d \ll v_s$, where v_s is the shock velocity, then we may neglect the photon diffusion. In this case the radiation moves with the matter; its effects on the dynamics can be represented by merely including a radiation pressure and energy in the equation of state. A shock with spherical symmetry must be followed by a rarefaction wave to ensure mass conservation. Matter flowing into the shock is compressed and then expanded by the rarefaction wave. We can identify the width of this high-density "spike" with the characteristic scale ΔR introduced above. In a medium of initially uniform density the fluid velocity just behind a strong shock falls off like $u_s \propto r_s^{-3/2}$, where r_s is the shock radius (see Landau and Lifshitz 1959). The flow approaches a similarity solution. The shock thickness is proportional to r_s and the density increase across the shock is constant so that the energy density in the shock decreases with time ($\rho u^2 \propto r_s^{-3}$). The distribution of velocity in the fluid behind the shock, as a function of radius, depends on the equation of state, but roughly

$$u/u_s \propto r/r_s\,.$$

Once the shock has passed, the outlying elements of matter are expanding fastest.

While much of the envelope of an extended supergiant might be approximated (roughly) by a uniform-density sphere, a decrease in density invariably occurs at the surface. If the density decreases to zero according to a power law

$$\rho_{00} = bx^\delta$$

(notation here follows Zel'dovich and Raizer 1967), where $x = R - r$ is the distance from some radius r to the surface at R and b and δ are constants, then an analytic solution can be found for strong shocks. When the shock reaches the surface ($r_s = R$), we have a fluid velocity

$$u \propto x^{-(1-\alpha)/\alpha}$$

and postshock density $\rho \propto x^\delta$. Now in general the constant α depends on δ and on the equation of state. Here it turns out that $\alpha < 1$; we will take $\alpha = \frac{1}{2}$ for illustration. Then the energy density $\rho u^2 \propto x^{\delta-1} \approx x^2$ roughly, which decreases to zero as $x \rightarrow 0$. The increase in u near the surface is sometimes called shock "acceleration."

This suggests that a decreasing density gradient near the stellar surface will cause larger postshock velocities than the uniform-density solution would predict. Crude zoning suppresses the effect of a density gradient; consequently it is not surprising that the dashed portion of the curve in Figures 3 and 4 is lower than it should be. Subsequent calculations (Falk and Arnett 1976) show that these arguments are indeed correct; even with the zoning still not optimal, peak velocities at $\tau = 1$ of above 6000 km s^{-1} were found. We present the original predictions here; with this mathematical blemish removed, a better agreement with the observational data would result. The velocities before $t \approx 20$ days would still be a bit low, however (see below).

Finally, note that because the density does decrease near the surface the condition $v_d \ll v_s$ must be violated at some point. Because $\lambda = 1/\rho\kappa$, we have

$$v_d = c/3\Delta R\rho\kappa\,.$$

For an energetic shock the opacity κ is approximately that for Thomson scattering on free electrons. As the surface is approached, $\Delta R\rho$ must become small, and v_d large. Even if v_s is as low as 10^3 km s^{-1}, $v_s \approx v_d$ implies $\Delta R/\lambda \approx 10^2$ while $v_s \approx c$ implies $\Delta R \approx \lambda$. Although the similarity solutions break down under these conditions our method of calculating radiative transfer is probably adequate (Falk and Arnett 1976).

d) *Acceleration by Photon Flux*

Consider a strong shock propagating through the extended envelope of a supergiant. Behind the shock front almost all of the internal energy is contributed by the radiation field. The acceleration of matter by this radiation is given by

$$a = \kappa F/c\,.$$

In the optically thin case,

$$\kappa F = \sum_{\nu} \kappa_\nu F_\nu \,,$$

where the subscript ν refers to a frequency band and the summation is over all the bands which make up the spectrum. Thus if $F = L/4\pi r^2$ is the energy flux, then κ is the flux-weighted mean opacity. In the optically thick case,

$$F = -\frac{\lambda c}{3}\frac{d}{dr}(aT^4) \,,$$

$$= \left(-\frac{1}{\rho}\frac{dP_{\rm rad}}{dr}\right)\frac{c}{\kappa} \,,$$

so that we have

$$a = -\frac{1}{\rho}\frac{dP_{\rm rad}}{dr} \,,$$

which is the usual result. In this case κ is the Rosseland mean opacity. In the numerical examples that follow we will take $\kappa = 0.4\ {\rm cm}^2\ {\rm g}^{-1}$.

Suppose the luminosity occurs in a short burst at time $t = 0$, so that $L = E_b\delta(t)$ and $E_b = \int L dt$ is the total photon energy radiated in the burst. Then the change in the fluid velocity of the matter is

$$\Delta v = \int a dt = \kappa E_b / 4\pi c {r_0}^2 \,,$$

where r_0 is the initial radius of the matter. In units typical of our models we have

$$v - v_0 = 10^9\ {\rm cm\ s^{-1}}(E_b/10^{49}\ {\rm ergs})(10^{14}\ {\rm cm}/r_0)^2 \,.$$

This solution is incomplete because the burst energy E_b must still be determined. Using computer calculations we can relate E_b to the total explosion energy E_t. More extended models radiate more efficiently. For $r_0 \lesssim 10^{15}$ cm we find

$$f = E_b/E_t \approx 0.006(r/10^{14}\ {\rm cm})^{7/4}$$

for a series of fairly realistic models (see Falk and Arnett 1976 for details). We do not yet know if drastically different structure, composition, etc., would give results that are significantly different in this sense. At present this expression should be considered as an example, not as a general result. In this case we have

$$v - v_0 = 6{,}000\ {\rm km\ s^{-1}}(E_t/10^{51}\ {\rm ergs})(10^{14}\ {\rm cm}/r_0)^{1/4} \,,$$

which is not so sensitive to r_0.

Observed supernovae often exhibit a burst in luminosity followed by a slower decline. Consider the acceleration of matter if the luminosity is constant. Then

$$a = \frac{\kappa}{c}\frac{L}{4\pi r^2} \,;$$

and if κ is constant and we multiply both sides by the velocity v and integrate, we find

$$\tfrac{1}{2}(v^2 - {v_0}^2) = \frac{\kappa L}{4\pi C r_0}\left(1 - \frac{r_0}{r}\right) \,.$$

If $v_0 = 0$ and $r \gg r_0$ we have

$$v = 4{,}500\ {\rm km\ s^{-1}}(L/10^{43}\ {\rm ergs\ s^{-1}})^{1/2}(10^{14}\ {\rm cm}/r_0)^{1/2} \,.$$

If there has been acceleration by an initial burst, v_0 may not be negligible, and a larger final velocity would result.

This simple analysis illustrates why the detailed numerical models work and is useful for making rough estimates. They are reasonably accurate for the bulk of the star but near the surface the burst energy E_b (or L) depends on details of the shock behavior in the density gradient.

We now return to the problem of the Doppler shifts of absorption lines shortly after maximum ($t \lesssim$ 20 days). The good agreement for velocity and rate of change in velocity for later times ($t \gtrsim$ 20 days with better zoning) indicates that the velocity field for this matter is correctly predicted. Most of the mass and energy reside in this material. However, for earlier times (at $t \approx 10$ days) the predicted velocity is low by a factor of about $9/6 = 1.5$ (see Figs. 3 and 4). If this is not due to (1) observational problems or (2) an inadequate theoretical treatment of shock emergence, it could be due to (3) the choice of physical parameters for model A. The analysis above suggests that increasing E_t or L by a factor of 2 or 4, or decreasing the initial radius r_0 from 1.6×10^{14} cm to, say, 5×10^{13} cm would increase the peak velocities to around 9,000 km s^{-1} for deep ($\tau = 1$ in continuum) lines. More recent calculations (Falk and Arnett 1976) support this suggestion. These changes are not large: it is not yet clear which of them (if any) are needed.

e) *Radius of the Photosphere and Supernova Distances*

If the apparent luminosity and the effective temperature of a supernova are measured, and its distance known (from identification of its parent galaxy, for example), then its photospheric radius $R_{\rm ph}$ is determined. A sequence of observations give $R_{\rm ph}$ as a function of time. The photospheric radii for SN 1969l as determined by the data of Ciatti, Rosino, and Bertola (1971) and Kirshner and Kwan (1974) are shown in Figure 5. The theoretical predictions (model A) are shown as solid lines.

Initially the radius of the photosphere $R_{\rm ph}$ is just the radius of the outer zone R; after being accelerated as the shock reaches the stellar surface, this zone coasts at almost constant velocity. As expansion increases transparency, the photosphere (here defined as the radius at which optical depth $\tau = 1$) moves inward in mass so that $R_{\rm ph}$ does not increase as fast as R. At $t \approx 4 \times 10^6$ s the effective temperature has dropped to 7000 K; recombination begins to reduce the Rosseland opacity. For computational reasons

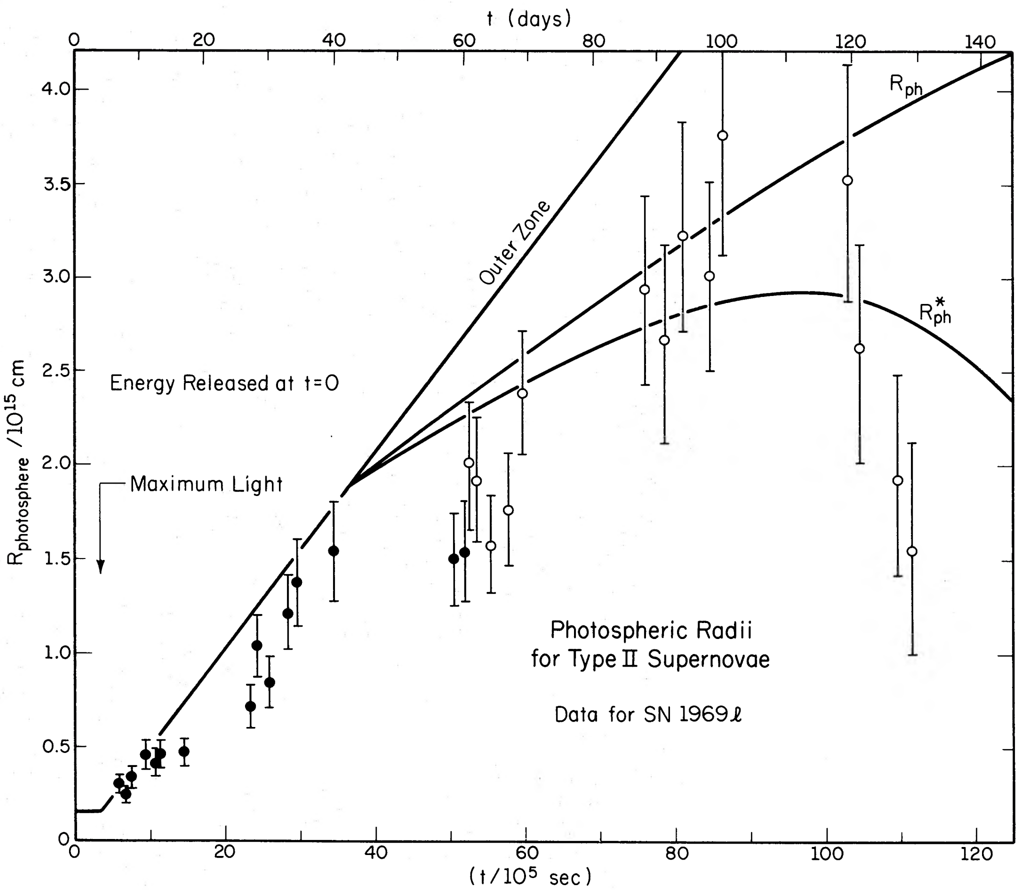

FIG. 5.—Photospheric radii for Type II supernovae. Notation for the source of the data points is as in Fig. 1. Distance to SN 1969l was taken from Kirshner and Kwan (1974). The solid curves are from model A. Besides the radius of the outer zone, also shown are the radius at $\tau = 1$ for two assumptions about the effective opacity at low temperature. The curve labeled with an asterisk (PHOTOSPHERE*) corresponds to a Population I composition and Rosseland mean opacity. The other curve (PHOTOSPHERE) is the same except the opacity was not allowed to fall below 0.1 of the Thomson value. The photospheric radius probably decreases after $t \approx 10^7$ s, but the observational data are more uncertain at these later times.

we did not allow the opacity to drop below one-tenth the Thomson value (our time step was roughly proportional to opacity). This gave the curve labeled "photosphere." In order to illustrate the way in which the predictions of photospheric behavior depend on the opacity used, another radius R_{ph}* is shown (labeled with an asterisk). This is the photospheric radius that would have been obtained if no minimum was forced on the opacity.

As more matter becomes transparent, it becomes more difficult to relate these calculations to the observations. A time-dependent, extended spherical atmosphere is hard to compute. It becomes difficult to abstract the continuum from the increasingly prominent lines, and thus observe the photosphere. The increased size of the error bars reflects this trend. In view of these problems with the observations and the theory, the agreement is probably better than we should expect.

In converting the observational data to cgs units (i.e., actual linear scales) we have simply accepted the distance preferred by Kirshner and Kwan (1974). The error bars reflect uncertainties in the distance as well as in effective temperature. Another approach would be to use the theoretical model to infer a best self-consistent distance. From Figure 5 it is clear that such a distance estimate would be in agreement with (but perhaps slightly larger than) the estimate of Kirshner and Kwan (1974).

If we can establish the correctness of this physical picture by improvements in theory and observation, then we can better infer the distance of well observed supernovae of Type II. Because of their self-consistency and more fundamental nature, these calculations already provide a better underlying model for analysis of the sort given by Kirshner and Kwan (1974). Some further improvements are already being made.

The observational method of Kirshner and Kwan (1974) is limited to the early epoch of the expansion (before the photosphere has receded markedly in mass coordinate). They must assume that the velocity structure is homologous ($v \propto r$ at a given time), which is an approximation and ignores possible variations in individual events. However, for better accuracy it would be desirable to lengthen the baseline in time. As this method essentially determines an effective time derivative by finite differences, it is desirable to use as many data points over as wide a range in times as is possible.

A simple version of the procedure we propose is as follows: (1) calculate a set of theoretical models (e.g., model A, etc.), (2) reproduce effective temperature as a function of time (see Fig. 1), (3) reproduce Doppler shifts of absorption lines as a function of time (see Figs. 3 and 4), and (4) use the predicted absolute luminosity and observed apparent luminosity to determine the distance. This differs from the Kirshner and Kwan procedure in that it *self-consistently* relates the effective temperatures to the fluid velocities. An advantage of the theoretical approach is that it can be extended to directly relate detailed photometry to absolute luminosity for individual supernovae.

Even after $t \approx 1.2 \times 10^7$ s ≈ 5 months, only 1.5 $M_\odot$ of model A had become transparent (i.e., lay outside $\tau = 1$; see Falk and Arnett 1976). Unless there was mixing of synthesized matter prior to explosion or a pronounced Rayleigh-Taylor instability between mantle and envelope (not seen in model A), this matter would have the composition of a supergiant envelope, not a core. *The bulk of matter processed by thermonuclear reactions does not necessarily appear at the photosphere during the observationally favorable stage of the explosion* (see Arnett 1969 and 1971; Falk and Arnett 1973; Kirshner and Kwan 1975).

The earliest data in Figure 5 suggest that initially the photospheric radius was $R_{\rm ph} \leqslant 3 \times 10^{14}$ cm. The absence of an observed presupernova leads Kirshner and Kwan (1974) to suggest $R_{\rm ph} \leqslant 10^{14}$ cm. This is an important result. First, it would rule out model B and other very extended presupernova structures for this *particular* event. Second, it suggests a way of testing theoretical ideas of the structure of the exploding star. At present the constraints are not strong, so for simplicity only a crude version of the argument will be given.

Stars of mass above $M/M_\odot \geqslant 3$ become as luminous as about $10^5 L_\odot$ (Paczynski 1969). Because of rapidly decreasing opacity stars do not have effective temperatures below, say, 2500 K. Thus the radius would be

$$R \approx (L/4\pi\sigma T_e^4)^{1/2} \approx 8 \times 10^{13}\ \text{cm} .$$

This is very close to Kirshner and Kwan's upper limit. For smaller stars, adiabatic cooling occurs before transparency and the explosion energy goes into mass motion (Colgate and White 1966). If instead we take $R_{\rm ph} \leqslant 3 \times 10^{14}$ cm, the argument gives $L \leqslant 10^6 L_\odot$. On the basis of luminosity alone this would imply a helium core mass $M_\alpha \leqslant 24\, M_\odot$ or a main-sequence mass of about $M \leqslant 60\, M_\odot$. It is not clear whether very massive stars $M \geqslant 30\, M_\odot$ ever become red supergiants; although they have the required luminosity, they may not develop the large radii necessary. For $R_{\rm ph} \leqslant 10^{14}$ cm we have $M_\alpha \leqslant 8\, M_\odot$ or $M \leqslant 24\, M_\odot$; such stars may become red supergiants. Thus we have, on the basis of this model for this event, $3 \leqslant M/M_\odot \leqslant 30$, a crude but interesting result. If we had definitive data on the rising part of the initial burst, we could derive the radius of the star when it exploded. Using envelope calculations, the luminosity of the presupernova star could be derived, and consequently its *core* mass estimated. Unfortunately, much of the energy in the burst would probably be in the hard-ultraviolet which would make difficult an accurate estimate of effective temperature, at least by ground-based observations. By carefully fitting the observed T_e, L, and velocities, the *envelope* mass might be inferred. Such a test of the theory of late stages of stellar evolution would be valuable. Because of the rapid decrease in the initial mass function with increasing mass, the *typical* supernova by number would correspond to the lightest stars which become supernovae.

III. CONCLUSIONS

a) Theoretical Improvements

Since these calculations were done, some improvements have been made and others can be accomplished. Introduction of multi-group transport in the P_1 approximation allows a better representation of the spectrum (Falk and Arnett 1976). This allows a good representation even at small optical depths and (if one pays the price) of fluxes in important frequency bands.

An obvious improvement would be a *set* of calculations with consistent physics but many variations in preexplosion structure, composition, energy, and mass, for example. These calculations are expensive however, and we have only begun such a survey.

b) Observational Improvements

We wish to stress the importance of overlapping observations of the type accomplished by the Assiago and Caltech groups on SN 1969l. The early period ($t \leqslant 60$ days) is especially vital because there the theory is sufficiently simple that we may hope to calculate it correctly. Here comparison with observation will probably be most fruitful.

In particular, *what is the width of the initial burst of a Type II supernova*? Do they vary from event to event? Does assumed incompleteness in the data cause us to think curves like model A in Figure 2 are actually like model B with the earlier points missed? In what fraction (if any) of supernovae of Type II can we rule out curves like model A?

c) Implications

In these comparisons of the theoretical models and observations we have adjusted only one parameter (to synchronize the time scales). Considering the simplicity of the physical model and the difficulty of the observations, the agreement is superb. Even so, there are several mathematical improvements (discussed above) which will improve this agreement.

If this picture of the Type II supernova event withstands further tests by improvement in the theory and the observational data, to the extent we can regard it as correct, then it will allow us to learn more about presupernovae, about the supernova process itself, and about the distance scale of the Universe.

We wish to thank B. Paczynski for giving us copies of unpublished envelope calculations. This work was supported in part by NSF grants at Texas, Illinois, and Caltech.

REFERENCES

Arnett, W. D. 1969, in *Supernovae and Their Remnants*, ed. P. Brancazio and A. G. W. Cameron (New York: Gordon & Breach), p. 89.
———. 1971, *Ap. J.*, **163**, 11.
Chevalier, R. 1976, preprint.
Christy, R. F. 1964, *Rev. Mod. Phys.*, **36**, 555.
Ciatti, F., Rosino, L., and Bertola, F. 1971, *Mem. Soc. Astr. Italia*, **42**, 163.
Colgate, S. A., and White, R. 1966, *Ap. J.*, **143**, 626.
Cox, A. N., and Stewart, J. N. 1965, *Ap. J. Suppl.*, **11**, 22.
Falk, S. W. 1974, unpublished Ph.D dissertation, Astronomy Dept., University of Texas at Austin.
Falk, S. W., and Arnett, W. D. 1973, *Ap. J.* (*Letters*), **180**, L65.
———. 1976, in preparation.
Kirshner, R. P., and Kwan, J. 1974, *Ap. J.*, **193**, 27.
———. 1975, *Ap. J.*, **197**, 415.
Landau, L. D., and Lifshitz, E. M. 1959, *Fluid Mechanics* (Reading, Mass.: Addison-Wesley).
Paczynski, B. 1969, private communication: see also 1970, *Acta Astr.*, **20**, 47.
Zel'dovich, Ya. B., and Raizer, Yu. P. 1966, *Physics of Shock Waves and High-Temperature Hydrodynamic Phenomena*, Vol. **2** (New York: Academic Press).

W. David Arnett and Sydney W. Falk: Enrico Fermi Institute, University of Chicago, Chicago, IL 60637